

# Pulsed plasmas as a method to improve uniformity during materials processing

Pramod Subramonium<sup>a)</sup>

*Department of Chemical and Biomolecular Engineering, University of Illinois, 1406 West Green Street, Urbana, Illinois 61801*

Mark J. Kushner<sup>b)</sup>

*Department of Electrical and Computer Engineering, University of Illinois, 1406 West Green Street, Urbana, Illinois 61801*

(Received 13 February 2004; accepted 29 March 2004)

Continuous wave operation of inductively coupled plasma (ICP) reactors as used for materials processing and which have geometrical or flow asymmetries may produce asymmetric species densities, temperatures, and fluxes. Flow asymmetries that produce nonuniformities in plasma conductivity initiate a positive feedback loop. In this feedback loop, asymmetries in conductivity are reinforced by the resulting nonuniform power deposition, which causes electron impact ionization to also be nonuniform. In this article, we discuss results from a computational investigation of long-term transients during pulsed operation of ICPs and their consequences on side-to-side asymmetries in plasma properties. During pulsed operation, diffusion of charged species during the afterglow between pulses smoothens these asymmetries prior to the next power pulse. The power deposition during subsequent pulses is more symmetric and this reduces the positive feedback. The improvement in uniformity afforded by pulsing is determined by the intrapulse plasma dynamics, and so is a function of the pulse repetition frequency, duty cycle, and feedstock gas. Improvements in the azimuthal uniformity of reactant densities were obtained in Ar and Cl<sub>2</sub> plasmas in an asymmetrically pumped reactor using pulsed power. As dissociative attachment dominates in the afterglow of Cl<sub>2</sub> pulsed plasmas, it provides a more uniform sink for electrons compared to ambipolar diffusion and different systematic behavior is obtained compared to argon. © 2004 American Institute of Physics. [DOI: 10.1063/1.1751636]

## I. INTRODUCTION

Low electron temperature, high-plasma-density reactors are widely used for etching and deposition during microelectronics fabrication.<sup>1-5</sup> As the wafer size increases, the requirements for side-to-side uniformity and azimuthal symmetry become more stringent. Gas injection and pumping and their effects on process uniformity are well-characterized parameters in high pressure (>100 s mTorr) systems. However, the impact of the symmetry of gas injection and pumping on the uniformity of reactants is less well characterized in low pressure (<10 s mTorr) systems. Many of the inductively coupled plasma (ICP) systems used for etching and deposition have discrete nozzles or single sided asymmetric pumping.<sup>6,7</sup> These systems were designed assuming that at low pressure, transport is diffusion dominated and so the gas sources and sinks appear as volume averages. As such, their asymmetries should not adversely affect the uniformity of reactants to the substrate. However, previous experimental<sup>7,8</sup> and computational investigations<sup>9</sup> of ICP reactors show that asymmetric pumping may result in azimuthally asymmetric plasma parameters which ultimately translate to, for ex-

ample, nonuniform etch rates. The asymmetries produced by gas inlets, pumping ports, and nonuniform power deposition become more important as the wafer sizes become larger.<sup>10</sup>

Kim *et al.*<sup>7,8</sup> measured the radial and azimuthal variation of ion fluxes impinging on the wafer in ICPs sustained in Ar/SF<sub>6</sub> and Ar/Cl<sub>2</sub> using a two-dimensional (2D) array of planar Langmuir probes on a 200 mm Si wafer. The typical conditions were 200 W, flow rate of 200 sccm, and pressure of 10 mTorr. They observed that the ion fluxes had a maximum near the pump port, a condition that they attributed to reduced loss of charged species by recombination on the walls.

Khater *et al.*<sup>6</sup> investigated the uniformity of plasma density and etch rate in an ICP reactor having a single gas inlet producing a cross wafer flow. Typical conditions were 6 mTorr, SF<sub>6</sub>/Ar = 50/50, 700 W, bias of 50 W, and flow rates between 20 and 70 sccm. They found that etch rates varied by 30% along the direction of gas flow, but were uniform perpendicular to the gas flow. Langmuir probe measurements of ion saturation current showed that a plasma density gradient was sustained laterally across the reactor and as a function of height. These gradients were sustained despite the symmetric pumping and the relatively large mean free path of ions and radicals.

Panagopoulos *et al.*<sup>9</sup> developed a three-dimensional (3D) finite element fluid model to investigate azimuthal

<sup>a)</sup>Present address: Novellus Systems Inc., 11155 SW Leveton Dr., Tualatin, OR 97062; electronic mail pramod.subramonium@novellus.com

<sup>b)</sup>Author to whom correspondence should be addressed; electronic mail: mjk@uiuc.edu

asymmetries and their effects on etch uniformity in ICP reactors. Their conditions were 10 mTorr of  $\text{Cl}_2$ , 2000 W, and flow rate of 79 sccm. They observed that when etching is ion driven, the power deposition is the important metric for etch uniformity as azimuthal nonuniformities in electron impact sources can persist down to the substrate. They also observed that asymmetric pumping causes azimuthal variation in species densities.

In this article, results from a 3D computational investigation of pulsed operation of Ar and  $\text{Cl}_2$  ICPs with asymmetric pumping are discussed. Previous works on pulsed plasmas of interest to this work were recently reviewed.<sup>11,12</sup> We found that flow induced nonuniformities in species densities, and the plasma conductivity in particular, can feed-back through the resulting nonuniform power deposition. This feedback makes the electron impact sources asymmetric, which in turn reinforces the flow induced asymmetries. This positive feedback can be reduced by diffusion during the afterglow between pulses, which makes the subsequent power pulses more uniform. We found that pulsed operation with lower duty cycles and pulse repetition frequency (PRF) help reduce these flow induced asymmetries under select conditions.

A brief description of the parallel hybrid model used in this study is presented in Sec. II. The 3D dynamics of pulsed Ar and  $\text{Cl}_2$  plasmas are discussed in Secs. III and IV. Our concluding remarks are in Sec. V.

## II. DESCRIPTION OF THE MODEL

The model employed in this investigation is a moderately parallel implementation of the 3D Hybrid Plasma Equipment Model (HPEM3D).<sup>13</sup> HPEM3D is a modular simulation, which iteratively achieves a quasisteady state solution. The main body of HPEM3D consists of the electromagnetics module (EMM), the electron energy transport module (EETM) and the fluid kinetics module (FKM). The EMM calculates the inductively coupled electric and magnetic fields produced by the inductive coils. The EETM uses these fields to spatially resolve electron energy transport by solving the electron energy conservation equation. Electron transport coefficients and rate coefficients are obtained by solving Boltzmann's equation using a two-term spherical harmonic expansion. The electron impact source functions produced by EETM are used in the FKM during its next execution. The FKM solves separate continuity, momentum, and energy equations for all species coupled with Poisson's equation to determine the spatially dependent density of charged and neutral species, their fluxes and temperatures, and electrostatic fields. The densities produced by the FKM are used to calculate the plasma conductivity for the EMM and the collision frequencies for the EETM. These modules are then iterated to a quasisteady state (averaged over a rf cycle). When addressing pulsed operation, many power-on and power-off cycles are computed to achieve a pulse-periodic steady state.

In the computationally serial version of HPEM3D, each module receives updates from other modules at best once each iteration through the model. Although the short-term

transients (e.g., during one rf cycle) are separately captured in each module since the integration time resolves the rf period, the exchange of parameters on longer time scales is limited by the looping time between the modules. To adequately capture true transients, this looping time must be small compared to the time scale of the transients. However, in implementing such a strategy, the expediency of the serial hybrid technique is defeated.

To address these issues a computationally parallel implementation of HPEM3D has been developed. This is the 3D analog of the two-dimensional parallel version of the HPEM described (see Ref. 11). In the parallel HPEM3D, the EMM, EETM, and FKM are executed concurrently on separate processors of a moderately parallel computer using OPEN-MP directives.<sup>14</sup> In this approach the plasma parameters and electric fields from one module are made available "on the fly" in shared memory to be accessed by other modules on a real time basis. The frequent sharing of information between the three modules reduces the time lag between the individual modules. This aids in capturing the transient behavior of plasma properties during pulsed operation. The algorithms and methodology for parallelization are essentially the same as in the 2D model except that the electron energy equation is solved in the EETM instead of the electron Monte Carlo simulation.

In pulsed ICP systems, the rf power applied to the antenna is (square wave) modulated. The PRF is the number of power-on (active glow) and power-off (afterglow) modulation periods of the ICP power per second. The duty cycle is the fraction of a given modulation period that the power is on. The peak power is the maximum instantaneous power applied during the power-on portion of the pulse. Typical modulation parameters are PRFs of 10–100s of kHz and duty cycles of 30%–70%.

The computational approach for simulating pulsed operation was to specify a duty cycle, PRF, and either a peak rf power or a time averaged power. HPEM3D was then executed on a cw basis using the time averaged power to establish a steady state in electron and ion density, gas temperature, and gas flow field. Acceleration techniques are used during cw operation to speed the numerical convergence. Once the steady state is reached, the numerical acceleration is turned off and the power is pulsed at the specified PRF and duty cycle. The ramp up interval to the peak power is 5  $\mu\text{s}$ . The ramp down interval to the power-off state during the afterglow is 15  $\mu\text{s}$ . The power was actually reduced to  $5 \times 10^{-3}$  W during the afterglow and not set to zero due to numerical issues which require a nonzero power. The power during the off period is sufficiently low that no significant electron heating occurs. Successive pulses of on-and-off periods are computed until a pulse periodic steady state is achieved. This typically requires 4–10 pulses.

The effects of pulsed operation relative to cw operation on the uniformity of a given plasma parameter  $\phi(r, \theta)$  are quantified by factors  $\alpha$  and  $\beta$ .  $\alpha$  is a measure of the absolute rms deviation of  $\phi(r, \theta)$  from its azimuthal average,  $\eta(r)$ , which is then averaged over all radius

$$\eta(r) = \sqrt{\frac{1}{2\pi} \int_0^{2\pi} (\phi(r, \theta) - \bar{\phi}(r))^2 d\theta}, \quad (1)$$

where  $\bar{\phi}(r)$  is the azimuthal average

$$\bar{\phi}(r) = \frac{1}{2\pi} \int_0^{2\pi} \phi(r, \theta) d\theta. \quad (2)$$

The change relative to cw operation is then

$$\alpha = \frac{[\int_0^R \eta(r) r dr]_{\text{pulsed}}}{[\int_0^R \eta(r) r dr]_{\text{cw}}}. \quad (3)$$

$\alpha < 1$  implies improved uniformity during pulsed operation compared to cw operation.  $\beta$ , which is a relative measure of uniformity is normalized by the average value of  $\phi(r, \theta)$ :

$$\beta = \frac{\left[ \int_0^R \left( \frac{\eta(r)}{\bar{\phi}(r)} \right) r dr \right]_{\text{pulsed}}}{\left[ \int_0^R \left( \frac{\eta(r)}{\bar{\phi}(r)} \right) r dr \right]_{\text{cw}}}. \quad (4)$$

$\beta < 1$  also implies improved uniformity during pulsed operation compared to cw operation.

### III. PULSED Ar INDUCTIVELY COUPLED PLASMAS

Pulsed Ar ICPs sustained in an asymmetric reactor were investigated. The reaction mechanism for Ar is discussed in Ref. 11. The reactor, schematically shown in Fig. 1, has azimuthally symmetric coils and gas injection, but an asymmetric pump port which occupies the  $60^\circ$  segment on the right-hand side of the  $(r, \theta)$  plane. The antenna consists of two nested annuli set on top of a dielectric window with uniform azimuthal conduction currents to eliminate asymmetries that may result from either transmission line effects or the shape of the antenna. The gas injection is through a showerhead placed below the coils.

cw operation in this reactor produces azimuthal asymmetries in plasma properties (power, electron source and  $[\text{Ar}^+]$ ) as shown in Fig. 2. The base case conditions are a pressure of 10 mTorr, cw power of 250 W at 10 MHz and flow rate of 50 sccm. Species densities are shown in the  $(r, \theta)$  plane at height-A (1 cm below the showerhead) and height-B (1 cm above the plane of the wafer) as indicated in Fig. 1(a). Sources for electrons and power deposition are shown at height-A.

Due to the asymmetric pumping, gas injected away from the pump port (stagnant zones) has, on the average, a longer residence time in the reactor compared to that injected closer to the pump port. The differences in the residence time can be 10s of ms for a gas flow rate of 50 sccm. The absence of the close-in wall near the pump port has two important consequences. First, the local diffusion length is longer for ions and excited states near the pump port, thereby reducing their losses by recombination on the wall. Second, the reduced rate of ion recombination due to the longer diffusion length decreases the source for neutrals from the walls following recombination. Since the diffusion time for ions from the bulk plasma to the walls is  $\approx 30 \mu\text{s}$ , which is much shorter

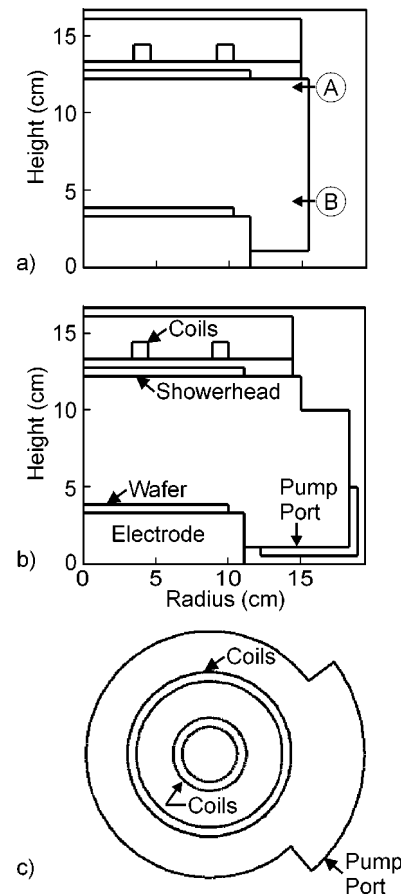


FIG. 1. Schematics of the asymmetric ICP reactor showing the showerhead and pump port locations. (a)  $(r, z)$  section through an azimuth of the reactor without a pump port. (b)  $(r, z)$  section through an azimuth with the pump port. (c) Top view of the reactor. The section markers show the heights at which plasma properties in the  $(r, \theta)$  will be shown. A symmetric reactor has the  $(r, z)$  section in (b) for full a  $360^\circ$ .

than the average residence time, the effective source of neutrals due to recombination at the walls can be commensurate to or exceed the net flow rate. In the base case, the source of neutrals on the walls resulting from ion recombination is approximately 50–100 sccm, commensurate with the injected flow rate. Due to the larger rate of recycling of neutrals and longer average residence time in the stagnant zones, the gas density is also larger in these volumes.

As the residence time is longer and neutral densities are larger in the stagnant zones, there is a greater likelihood for electron impact ionization and excitation reactions to occur further from the pump port. As a result, the specific energy deposition (eV/atom) is larger. This nonuniform source of ionization results in larger ion densities at sites that are remote from the pump. A second peak in the  $\text{Ar}^+$  ion density also occurs in the front of the pump port resulting from the reduced rate of recombination on the more distant walls, similar to the trends observed by Kim *et al.*<sup>7,8</sup> Depending on the details of the operating conditions, one of these two peaks may dominate.

As the electron density is azimuthally asymmetric, the plasma conductivity is also nonuniform. A nonuniform plasma conductivity produces nonuniform power deposition, which results in asymmetric electron impact sources, thereby

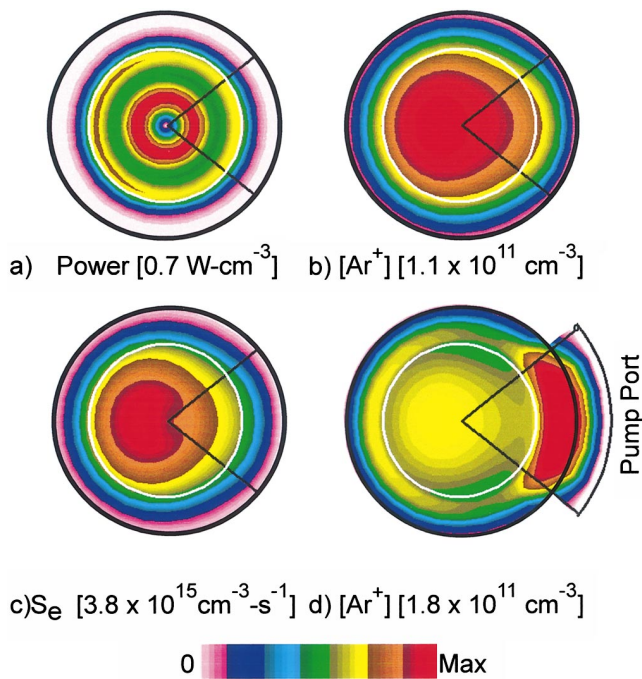


FIG. 2. (Color) Ar plasma properties for cw operation in an asymmetric reactor (10 mTorr, 250 W, 50 sccm). (a) Power deposition, (b)  $[Ar^+]$  below the dielectric (height-A). (c) electron impact ionization sources (d)  $[Ar^+]$  above the wafer (height-B). The white circle is the outline of the substrate. The maximum for each quantity is noted in the brackets. Nonuniform power deposition results in nonuniform electron impact ionization sources producing the maximum in ion density away from the pump port. The remoteness of the wall produces a maximum in  $[Ar^+]$  near the pump port.

reinforcing the asymmetries in species densities. Relatively small changes in gas density resulting from asymmetric pumping (or gas injection) can produce significant asymmetries in plasma properties by initiating this positive feedback loop. The magnitude (and sign) of the feedback loop results in part as to whether, for example, plasma densities increase or decrease with increasing gas density. For a constant power deposition in argon for the pressure ranges of interest (a few to 10s mTorr), the plasma density generally increases with pressure, which then produces a positive feedback loop.

It is our premise that these azimuthal asymmetries can be reduced, and the plasma uniformity improved, by limiting the positive feedback between nonuniform electron density and power deposition by using pulsed operation. With pulsed operation, electron impact sources for high threshold events (such as ionization) greatly decrease (or are eliminated) during the afterglow periods thereby temporarily eliminating the positive feedback. The diffusion of charged and excited species during the afterglow smoothens the nonuniformities created during the previous power pulse, thereby providing more uniform initial conditions for the next power pulse.

To investigate this premise, parameterizations were performed for pulsed Ar ICPs by varying the duty cycle and PRF. The base case conditions were 10 mTorr, 50 sccm, a peak power of 500 W modulated at a PRF of 10 kHz and a duty cycle of 50% (average power 250 W). As a point of reference, reactor averaged electron density ( $n_e$ ) and electron temperature ( $T_e$ ) as a function of time for duty cycles of

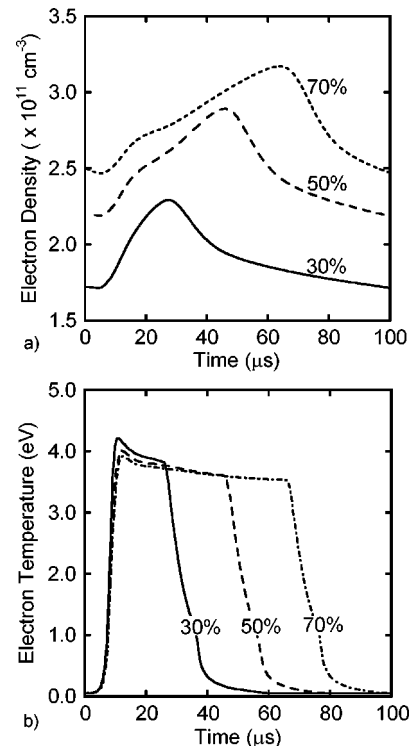


FIG. 3. Reactor averaged plasma properties in Ar as a function of time for different duty cycles for a constant peak power of 500 W, PRF of 10 kHz, and gas flow of 50 sccm. (a) Electron density and (b) electron temperature.

30%, 50%, and 70% are shown in Fig. 3. The average power depositions are 150, 250, and 375 W. (More extensive characterizations of pulsed Ar plasmas can be found in Ref. 11, and references therein.) During the activeglow the electron density ramps up from its low value at the end of the previous afterglow period. For these conditions, the duration of the activeglow is not sufficient to achieve a quasisteady state even for a duty cycle of 70%. As such, the reactor averaged electron densities at the end of the activeglow increase with increasing duty cycle reflecting the increase in average power ( $2.2 \times 10^{11} \text{ cm}^{-3}$ ,  $2.8 \times 10^{11} \text{ cm}^{-3}$ , and  $3.2 \times 10^{11} \text{ cm}^{-3}$  for duty cycles of 30%, 50%, and 70%). Following termination of power, the electron and ion densities decay by diffusion and recombination on the walls. For these conditions, the diffusion is dominantly ambipolar for the entire afterglow period. Smaller PRFs or shorter duty cycles may produce afterglow periods which are sufficiently long that charged particle loss transitions from ambipolar to free diffusion.

As the ICP power is turned on, the electrons that survive the afterglow of the previous pulse are accelerated by the inductive fields. During the initial stages of the power-on ramp, this power is dissipated into a smaller inventory of electrons surviving the previous afterglow. As a consequence,  $T_e$  spikes to 4.2 eV, compared to the steady state value of 3.6 eV, to enable the smaller inventory of electrons to dissipate the desired power. (Power dissipation per electron generally increases with increasing  $T_e$ .) The higher  $T_e$  also produces an electron avalanche thereby increasing the plasma density. Shorter duty cycles produce smaller electron densities at the end of the longer afterglow (for example,

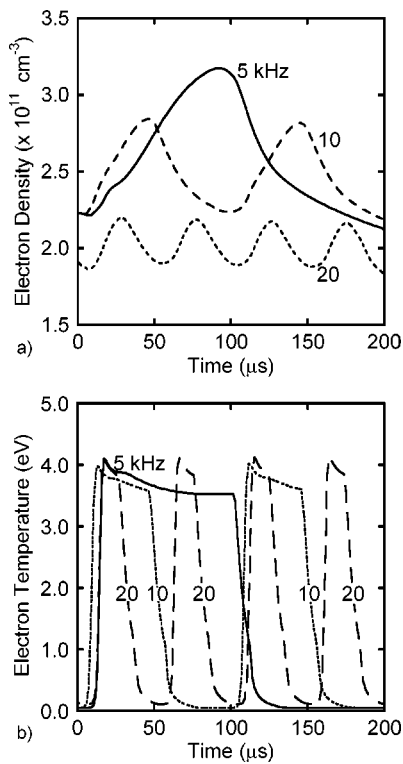


FIG. 4. Reactor averaged plasma properties in Ar as a function of time for different PRFs for a constant peak power of 500 W, duty cycle of 50% and gas flow of 50 sccm. (a) Electron density and (b) electron temperature.

$n_e = 1.7 \times 10^{11}$  and  $2.5 \times 10^{11} \text{ cm}^{-3}$  at the end of the afterglow for duty cycles of 30% and 70%). As a result  $T_e$  spikes to a higher initial value with smaller duty cycles. As the electron density increases in the activeglow, the ICP power is dissipated into a larger inventory of electrons allowing the electron temperature to decrease. As a balance is reached between ionization and loss processes in the late activeglow,  $T_e$  reaches a quasisteady state value of 3.6 eV for duty cycles  $>50\%$ . For shorter duty cycles the active glow is not long enough to attain this balance and  $T_e$  declines to, for example, only 4 eV for a duty cycle of 30%.

When the power is turned off,  $T_e$  rapidly falls as electrons cool by inelastic collisions dominantly with Ar metastables. The rate of inelastic collisions is higher during the initial stages of the afterglow as the Ar metastable density ( $4.5 \times 10^{11} \text{ cm}^{-3}$ ) and the power dissipation per electron are high. However, as the electrons cool and their rate of power dissipation decreases, in this case after about 15  $\mu\text{s}$  into the afterglow, the rate of decay of  $T_e$  also decreases. At lower duty cycles, the afterglow is long enough that the electrons essentially thermalize with the gas.

The reactor averaged  $n_e$  and  $T_e$  for PRFs of 5, 10, and 20 kHz for a 50% duty cycle (but otherwise the base case conditions) are shown in Fig. 4. For a fixed duty cycle and constant average power, higher PRFs produce shorter on-and-off periods. For a PRF of 5 kHz, the power-on period is nearly long enough to achieve a steady state electron density of  $3.2 \times 10^{11} \text{ cm}^{-3}$ . At higher PRFs the power-on time is not sufficient for the electron density to reach this quasisteady state value within a given pulse. A periodic steady state is,

however, achieved. The smaller electron density at the end of the longer afterglows with smaller PRFs produces a larger initial  $T_e$ , resulting in more efficient ionization. As a result, the time averaged  $n_e$  generally increases with decreasing PRF. For example, the time averaged  $n_e$  is 2.1, 2.5, and  $2.7 \times 10^{11} \text{ cm}^{-3}$  for 20, 10, and 5 kHz.

The consequences of pulsing on flow induced asymmetries will be quantified by first operating the reactor on a cw basis using the same average power to obtain a base line, followed by a series of power pulses. Plasma properties averaged over a pulse period will then be inspected for successive pulses. Pulse averaged  $[\text{Ar}^+]$  for pulses 2–5 following cw operation of the base case are shown in Fig. 5. (The cw values are shown in Fig. 2.) During cw operation, the peaks in  $[\text{Ar}^+]$  below the dielectric ( $1.1 \times 10^{11} \text{ cm}^{-3}$ ) and above the wafer ( $1.3 \times 10^{11} \text{ cm}^{-3}$ ) are offset  $\approx 2.5 \text{ cm}$ , from the center of the wafer to the side opposite the pump port. This offset is ultimately due to the higher specific energy deposition resulting from the longer residence time in that portion of the reactor. This peak in ion density shifts to the center of the reactor over a period of several pulses, thereby improving azimuthal symmetry.

This improvement in uniformity results from reducing the positive feedback between nonuniform plasma conductivity and power deposition. During the afterglow, the reduction in  $T_e$  rapidly quenches the asymmetric ionization processes, which would otherwise feedback to the power deposition by providing a nonuniform conductivity. The diffusion that then occurs during the afterglow mediates these nonuniformities during a time when there is no feedback to the power. At the end of the afterglow, species densities, and the conductivity in particular, are more uniform providing a more uniform set of initial conditions for the subsequent pulse. The power deposition during the next pulse is therefore more symmetric, which in turn improves the uniformity of electron impact sources. These effects play out over several pulses to make the plasma conductivity, power deposition, and reaction sources more uniform. As such, these intrapulse dynamics will depend on the length of the afterglow period during which the plasma properties are homogenized relative to the power-on period during which positive feedback produces asymmetries.

Power deposition and electron impact ionization sources below the dielectric (height-A) for pulses 2–5 following cw operation are shown in Fig. 6. Through several pulses, the sources and power deposition become more uniform as the positive feedback through the plasma conductivity is lessened. During cw operation, the peak in the ionization source ( $3.7 \times 10^{15} \text{ cm}^{-3} \text{ s}^{-1}$ ) is located  $\approx 3 \text{ cm}$  off center away from the pump port owing to power deposition and conductivity also peaking opposite the pump port. With successive pulses, the ionization sources become essentially azimuthally uniform. The remaining asymmetries at the wafer level in  $[\text{Ar}^+]$  then result from the geometrical effects of the pump plenum.

During cw operation, a peak in ion density ( $2.2 \times 10^{11} \text{ cm}^{-3}$ ) occurs near the pump port due to the longer diffusion length afforded by the pump plenum. As this geometrical asymmetry does not change with pulsing, this local

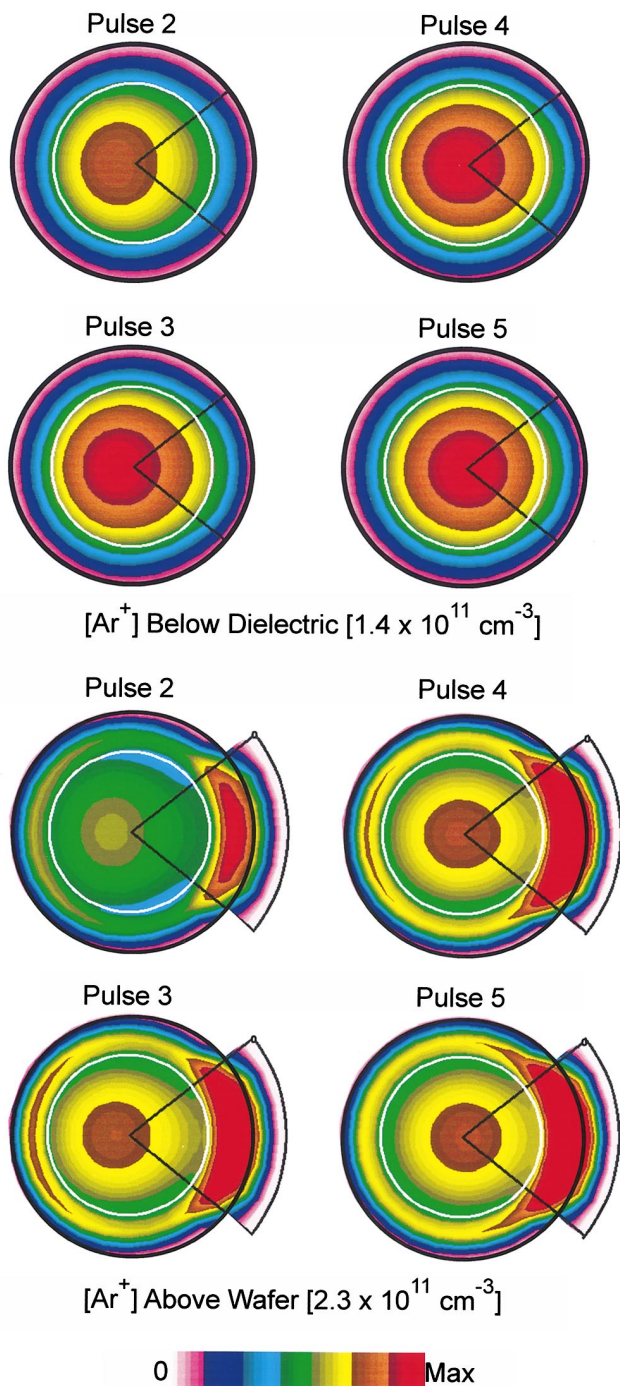


FIG. 5. (Color)  $[Ar^+]$  averaged over a pulse period for pulses 2, 3, 4, and 5 following cw operation (peak power 500 W, 10 mTorr, 50 sccm, PRF 10 kHz, duty cycle 50%). (a) Below the dielectric (height-A) and (b) above the wafer (height-B). The white circle is the outline of the substrate. The maximum for each set is noted in the brackets.  $[Ar^+]$  at both locations become more uniform with successive pulses following cw operation.

maximum in ion density remains even after several pulses. It is unlikely that pulsing alone will eliminate this asymmetry. Reactor designs without the pump port cavity but with asymmetric pumping can also have flow induced asymmetries. For these conditions pulsing alone may be more effective in reducing the asymmetries. For example,  $[Ar^+]$  and power deposition are shown in Fig. 7 for 300 W and 5 mTorr for a reactor without the pump port plenum but with asymmetric

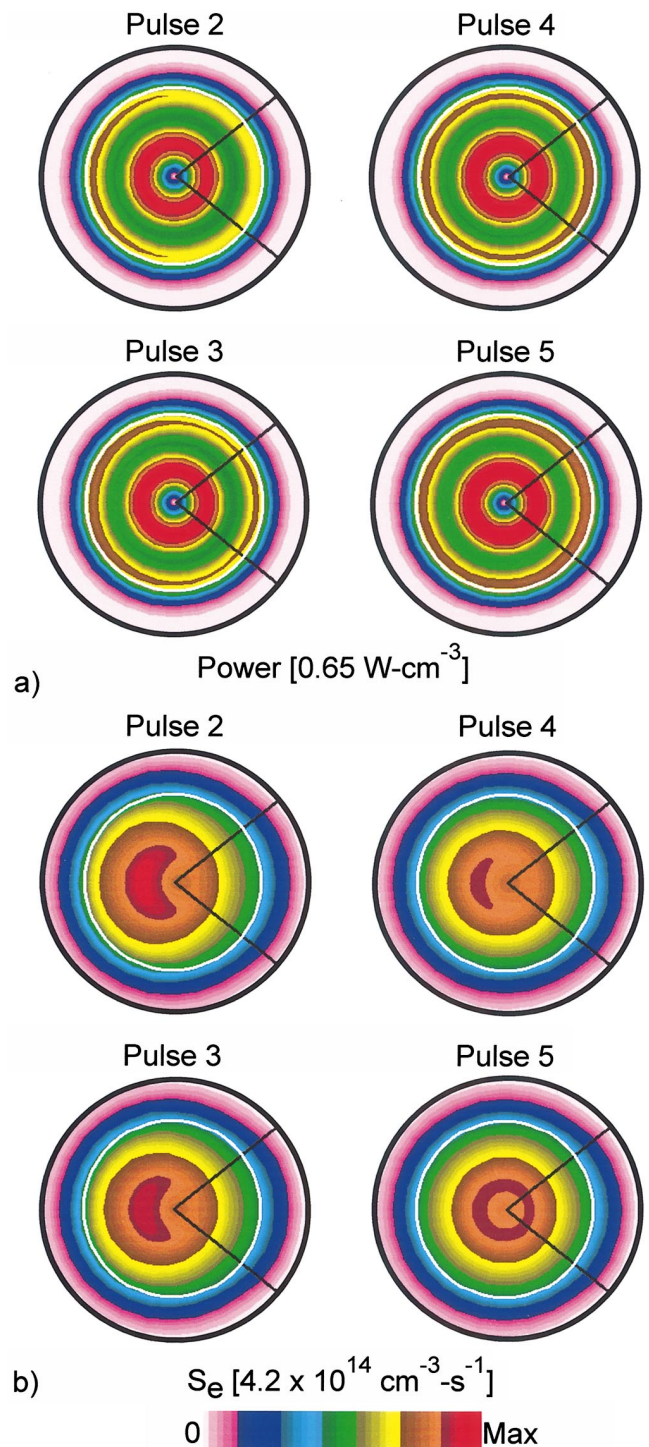


FIG. 6. (Color) Time averaged (a) power deposition and (b) electron impact ionization sources below the dielectric (height-A) for pulses 2, 3, 4, and 5 following cw operation (peak power 500 W, 10 mTorr, 50 sccm, PRF 10 kHz, duty cycle 50%). The white circle is the outline of the substrate. The maximum for each variable is noted in the brackets. The power deposition and electron impact ionization sources become more uniform with successive pulses following cw operation.

pumping in the same quadrant. Beginning from the cw conditions with a peak in  $[Ar^+]$  on the side of the reactor opposite the pump port,  $[Ar^+]$  and power deposition achieve essentially azimuthally symmetric profiles after several pulses.

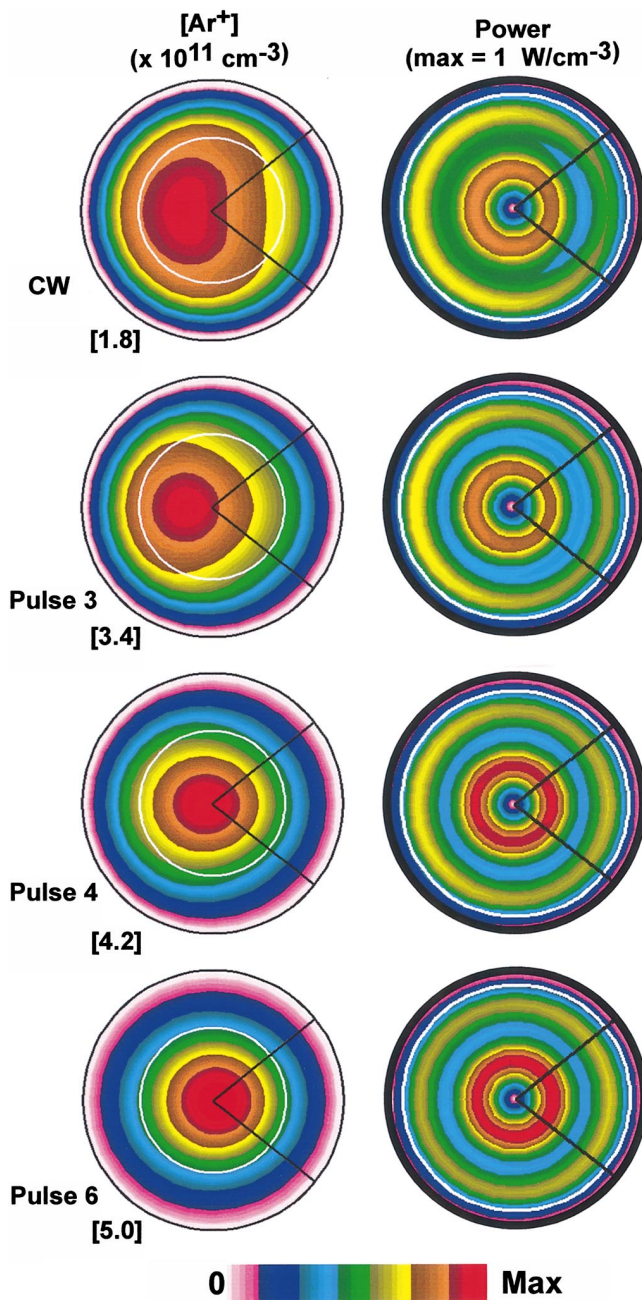


FIG. 7. (Color)  $[\text{Ar}^+]$  and power deposition for a reactor without a pump plenum but with asymmetric pumping (300 W, 5 mTorr, 160 sccm). Results are shown for cw operation, and pulse averages for 3, 4, and 6 pulses after cw operation for a PRF of 10 kHz and 50% duty cycle. The white circle is the outline of the substrate. The maximum for each frame for  $\text{Ar}^+$  is noted in the brackets (units of  $10^{11}\text{cm}^{-3}$ ).

$[\text{Ar}^+]$  at the end of six pulses following cw operation (averaged over a pulsed cycle) are shown in Fig. 8 for duty cycles of 30%–70% and an average power of 250 W. Power deposition and electron impact ionization sources are shown in Fig. 9. As the duty cycle is decreased for fixed PRF, the afterglow period is lengthened. The nonuniform electron impact sources produced by the positive feedback during the afterglow are therefore absent, and the mitigating diffusion is active, for a longer duration. The positive feedback during the power pulse also occurs for a shorter duration. On this basis alone, one should expect monotonic improvements in

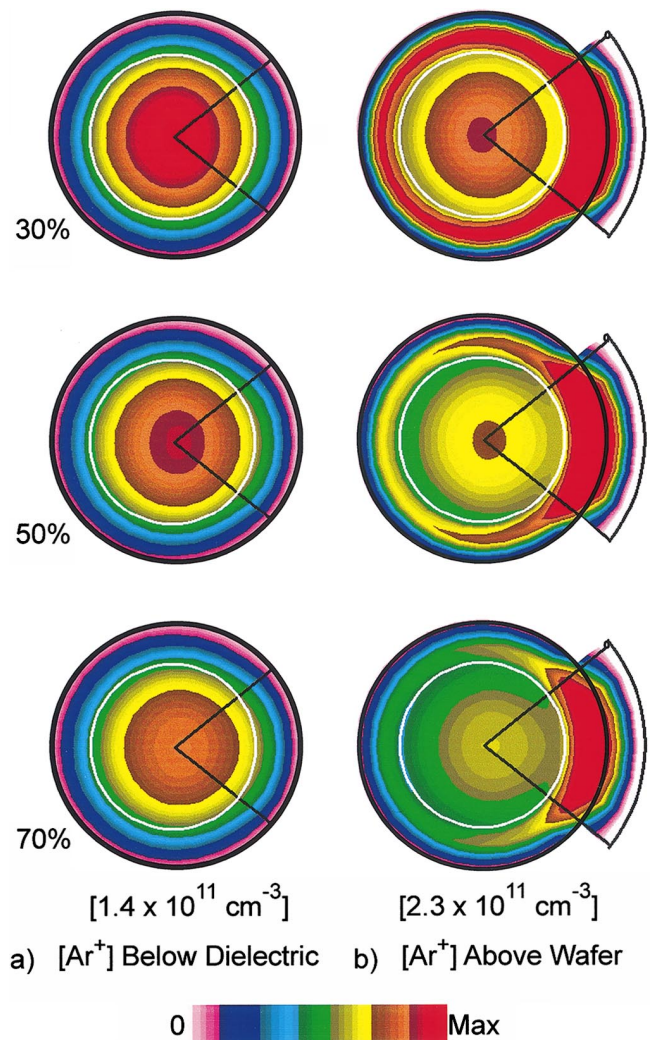


FIG. 8. (Color)  $[\text{Ar}^+]$  averaged over a pulse period at the end of six pulses following cw operation for duty cycles of 30%, 50%, and 70% (average power 250 W, 10 mTorr, 50 sccm, and PRF of 10 kHz). (a) Below the dielectric (height-A) and (b) above the wafer (height-B). The white circle is the outline of the substrate. The maximum for each column is noted in the brackets. Lower duty cycles for a better azimuthal symmetry as the longer afterglow enables diffusion to smoothen density profiles prior to the next power pulse.

uniformity with decreasing duty cycle. Having said that, to deposit the same average power with a shorter duty cycle, the peak power deposition during the activeglow must be larger. Previous studies have shown that the azimuthal uniformity of plasma densities generally decreases with increasing power due to there being an increased positive feedback.<sup>15</sup> Therefore, as the duty cycle decreases with constant average power, there is more positive feedback during the shorter power-on period (due to the higher peak power) and while there is more mitigating diffusion during the longer afterglow period. Hence, a nonmonotonic improvement in uniformity with duty cycle may occur as shown in Figs. 8 and 9. If instead the peak power is held constant while the duty cycle is lowered, the dominant effect is the lengthening of the afterglow with its mitigating diffusion. As a result, monotonic improvement in uniformity is expected.

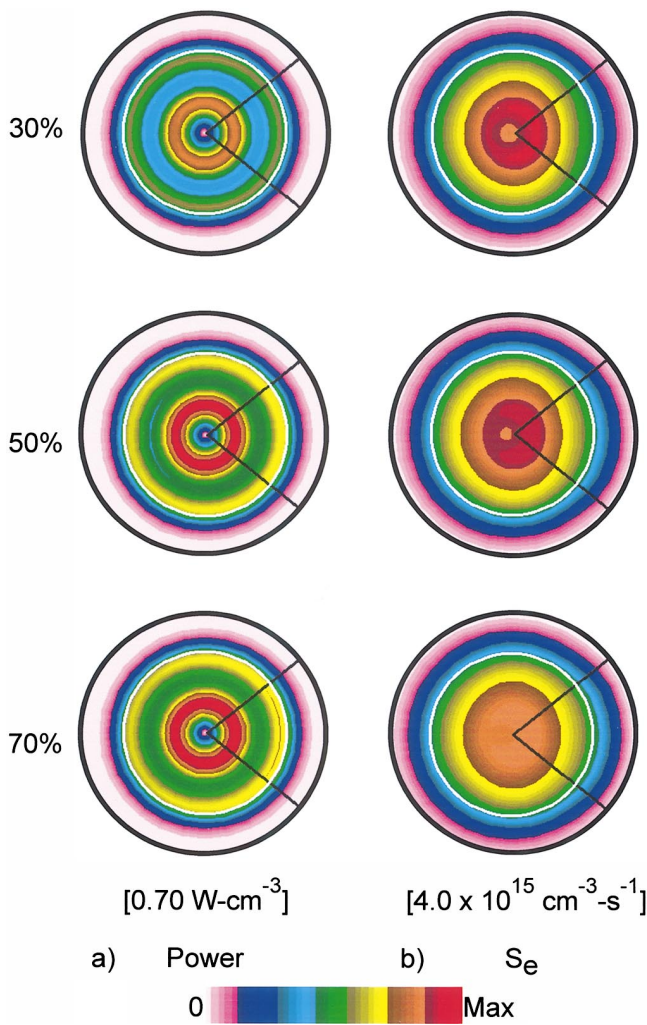


FIG. 9. (Color) Plasma parameters below the dielectric (height-A) at the end of six pulses following cw operation for duty cycles of 30%, 50%, and 70% (average power 250 W, 10 mTorr, 50 sccm, and PRF of 10 kHz). (a) Power deposition and (b) electron impact ionization sources. The white circle is the outline of the substrate. The maximum for each quantity is noted in the brackets. The uniformity of electron impact ionization sources improve by 40% for a duty cycle of 30%.

For a constant power of 250 W, the azimuthal uniformity of densities had nonmonotonic behavior from cw to lower duty cycles. For example,  $\alpha$  and  $\beta$  for  $[\text{Ar}^+]$  were 1.2 and 1.0 for a duty cycle of 70% and improved to 1.0 and 0.6 for a duty cycle of 30%. With  $\alpha > 1$ , the uniformity was actually worse for a duty cycle of 70% compared to cw operation. In this case, the larger ICP power (360 W) during the activeglow, which reinforced the positive feedback, produced nonuniformities that could not be mitigated during the short afterglow period. At lower duty cycles, in spite of the even higher peak power during the activeglow which more strongly reinforces the positive feedback, the uniformity was improved as the longer afterglow period was able to mitigate these nonuniformities. Improving uniformity using pulsed operation is then ultimately a tradeoff between intensifying the feedback during the power-on period and mitigating the resulting nonuniformities during the afterglow. As a consequence, the success of this method will ultimately depend on peak or average power deposition, PRF, and duty cycle. Those

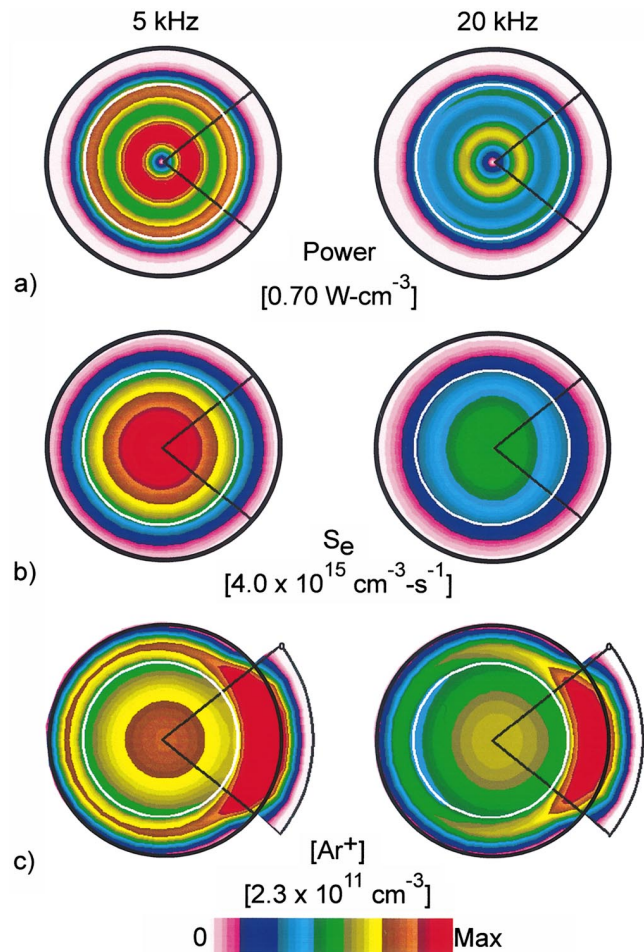


FIG. 10. (Color) Plasma parameters averaged over a pulse period at the end of six pulses for 5 and 20 kHz (average power 250 W, 10 mTorr, 50 sccm, and duty cycle of 50%). (a) Power and (b) electron source below the dielectric (height-A) and (c)  $[\text{Ar}^+]$  above the wafer (height-B). The white circle is the outline of the substrate. The maximum for each quantity is noted in the brackets. Lower PRFs result in better azimuthal symmetry.

dependencies will also be sensitive to gas mixture, pressure, and flow rates as these parameters determine the nature of the feedback.

It is not necessarily the case that the feedback during the activeglow is always positive. There are gas mixtures for which the efficiency of the net production of electrons (ionization minus attachment) decreases with increasing power deposition, and this could result in negative feedback. For example, the rate of dissociative attachment to  $\text{H}_2$  significantly increases as the molecule is vibrationally excited.<sup>16</sup> Local increases in power deposition which increase the density of  $\text{H}_2(v)$  will therefore decrease the net electron production efficiency by increasing the rate of attachment. The end result is negative feedback. Molecular gas mixtures in which dissociation products are more highly attaching than the parent gases will also show a similar effect.

The tradeoff between positive feedback during the activeglow and mitigation by diffusion during the afterglow was further investigated by varying PRF. For example, power deposition, ionization sources and  $[\text{Ar}^+]$  for PRFs of 5 and 20 kHz are shown in Fig. 10 for a 50% duty cycle. Since the duty cycle is fixed, the peak power during the

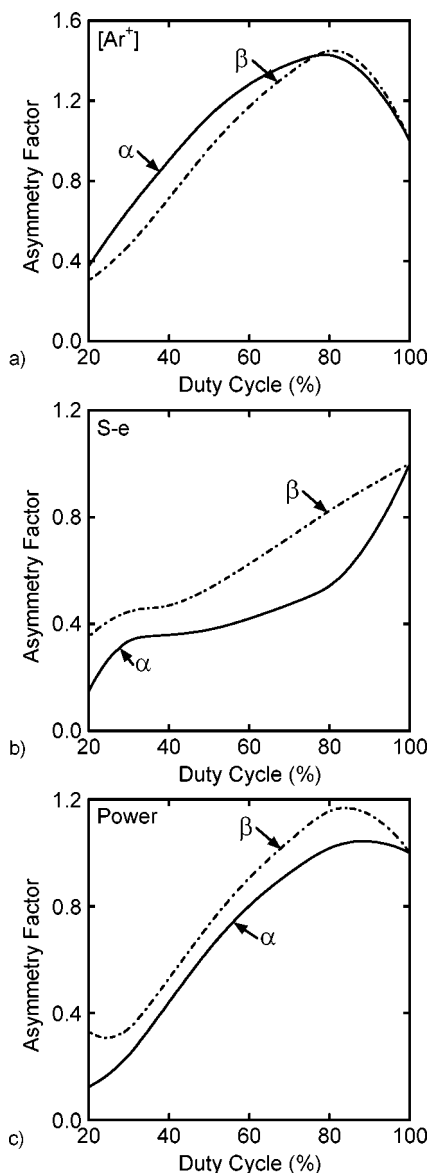


FIG. 11. The absolute ( $\alpha$ ) and relative ( $\beta$ ) asymmetry factor for (a)  $[\text{Ar}^+]$  above the wafer and (b) ionization sources and (c) power deposition below the dielectric as a function of duty cycle. The average power of 250 W was held constant (10 mTorr, 50 sccm, 10 kHz). Uniformity generally improves with decreasing duty cycle due to the longer afterglow and beneficial mitigating diffusion.

activeglow is constant and so the magnitude of the positive feedback is the same as the duty cycle is changed. However, as the PRF is decreased from 20 to 5 kHz, both the activeglow and afterglow are increased from 25 to 100  $\mu\text{s}$ , thereby increasing the duration of both the positive feedback and mitigation. For these conditions, the tradeoff between the longer activeglow that reinforces nonuniformities and the longer afterglow that reduces them is in favor of the afterglow, and so uniformity generally increased with decreasing PRF. In this regard, the uniformity of  $[\text{Ar}^+]$  improved by 15% when the PRF was decreased from 20 to 5 kHz. The uniformities of power deposition and ionization sources were also improved by 10% and 8%.

The consequences of duty cycle on asymmetries are quantified for an average power of 250 W in Fig. 11.  $\alpha$  (the

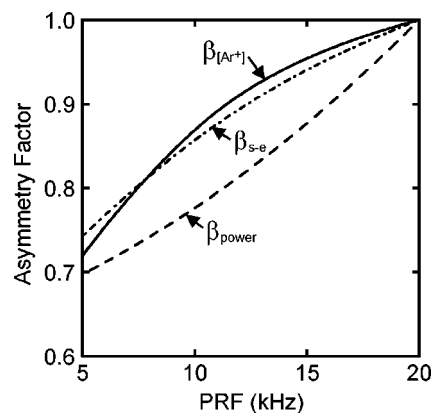


FIG. 12. The relative asymmetry factor  $\beta$  for  $[\text{Ar}^+]$ , electron impact ionization sources and power as a function of PRF (average power 250 W, 10 mTorr, 50 sccm). The asymmetry factor decreases with PRF.

absolute measure of uniformity) for  $[\text{Ar}^+]$  is nonmonotonic as the duty cycle is decreased. With decreasing duty cycle, the peak power during the activeglow must increase to maintain a constant average power that in turn increases the positive feedback.  $\alpha$  increases (less uniform) as the duty cycle is reduced to 80% as the tradeoff between increased feedback during the activeglow and the mitigating effects of diffusion favors the positive feedback. For lower duty cycles,  $\alpha$  decreases (more uniform) as the tradeoff between the longer afterglow offsetting the increased feedback during the activeglow is in favor of the diffusion.  $\beta$  (relative measure of uniformity) shows similar trends, increasing for small changes in duty cycle from cw operation, and decreasing with lower duty cycle. Similar trends are obtained for power deposition. Unlike the trends for  $[\text{Ar}^+]$  and power deposition,  $\alpha$  and  $\beta$  for electron impact ionization sources monotonically decrease with decreasing duty cycle. A more optimum chamber design would likely be able to take advantage of this scaling and achieve similar improvements for the ion density.

The effects of PRF (5–20 kHz) on asymmetries for  $[\text{Ar}^+]$ , ionization sources and power deposition are shown in Fig. 12 for a duty cycle of 50%. For a constant duty cycle, both the peak and average power remain constant with changes in PRF. Positive feedback during the activeglow may increase due to the duration of the activeglow at lower PRFs but not because of an increase in the magnitude of the power deposition. The relative asymmetry factor  $\beta$  decreases (becomes more uniform) in all cases due to the increase in afterglow period with decreasing PRF which allows the tradeoff to favor the mitigating diffusion.

#### IV. PULSED $\text{Cl}_2$ INDUCTIVELY COUPLED PLASMAS

In this section, the results from our computational investigation of  $\text{Cl}_2$  pulsed ICPs with asymmetric pumping are presented. The base case conditions are 10 mTorr, PRF of 10 kHz, duty cycle of 50%, peak ICP power of 300 W (average power of 150 W), and flow rate of 150 sccm. The reaction mechanism for  $\text{Cl}_2$  is discussed in Ref. 12. As a point of departure, power deposition, electron impact sources for electrons and Cl radicals, electron density, Cl density, and the positive ion density ( $\text{Cl}_2^+$  and  $\text{Cl}^+$ ) are shown in Fig. 13 for

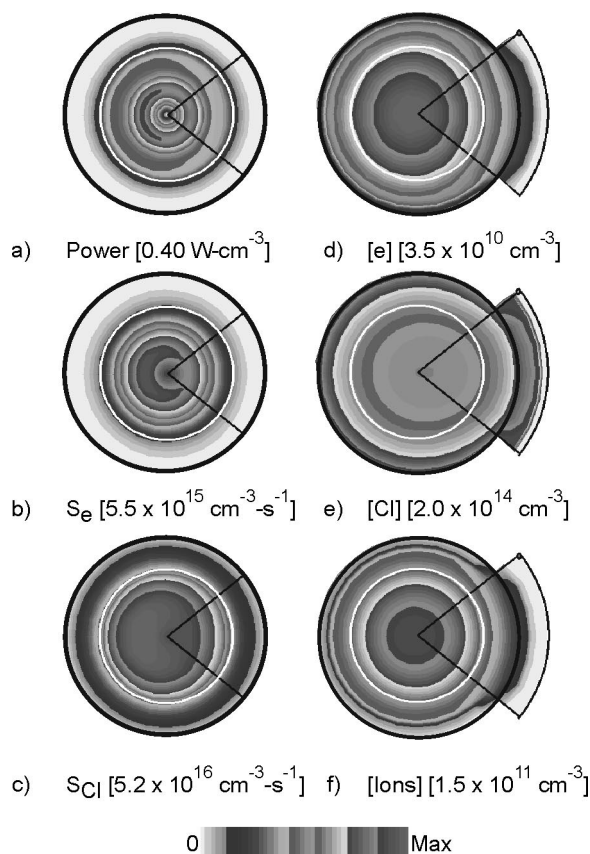


FIG. 13. Plasma properties for cw operation of a  $\text{Cl}_2$  plasma in an asymmetric reactor (10 mTorr, average power 150 W, 150 sccm). (a) Power deposition, (b) electron impact ionization sources, and (c) electron impact source of Cl radicals below the dielectric (height-A). (d) electron density, (e)  $[\text{Cl}]$ , and (f) positive ion density ( $[\text{Cl}_2^+] + [\text{Cl}^+]$ ) above the wafer (height-B). The white circle is the outline of the substrate. The maximum for each quantity is noted in the brackets.

cw operation in the asymmetric reactor. The ICP power deposition peaks at  $\approx 0.4 \text{ W/cm}^3$  below the inner coil opposite the pump port due to a local maximum in plasma conductivity. The power deposition produces asymmetric source functions, which produce maxima in the electron and ion densities away from the pump port. The peak positive ion density is  $\approx 1.4 \times 10^{11} \text{ cm}^{-3}$ .

The characteristics of pulsed  $\text{Cl}_2$  plasmas were recently reviewed in Ref. 12. A subset of relevant trends are discussed here. The reactor averaged electron density,  $\text{Cl}^-$  density and electron temperature as a function of time for different duty cycles are shown in Fig. 14. The dynamics of the electron density are in large part determined by electron impact ionization, whose rate coefficient increases with increasing  $T_e$ , and dissociative attachment



whose rate coefficient increases with decreasing  $T_e$ . When power is terminated at the end of the activeglow,  $T_e$  thermalizes within  $\approx 15 \mu\text{s}$ , a time determined largely by the inelastic collision frequency with  $\text{Cl}_2$ . The resulting increase in dissociative attachment produced a rapid decrease in  $n_e$ , and a corresponding increase in  $[\text{Cl}^-]$ . The maximum  $[\text{Cl}^-]$  occurs when its source is diminished by the depletion of elec-

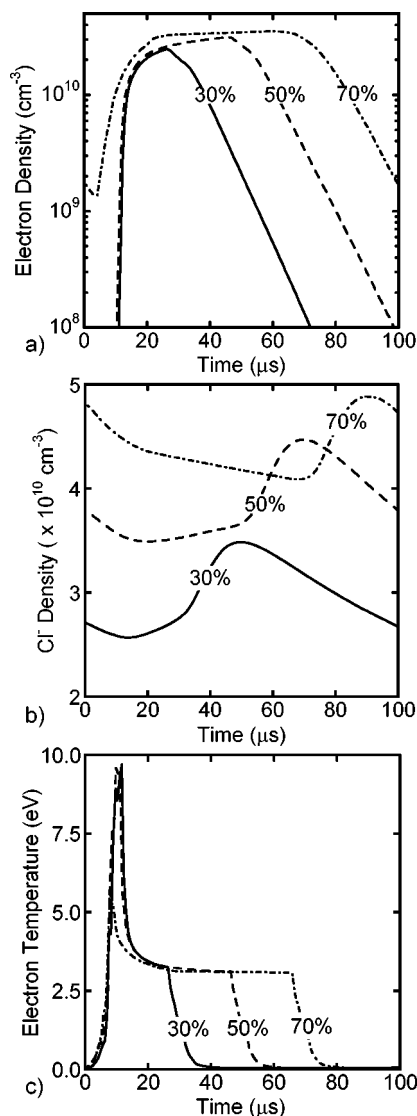


FIG. 14. Reactor averaged plasma properties in  $\text{Cl}_2$  as a function of time for different duty cycles for a constant peak power of 300 W, PRF of 10 kHz, and gas flow of 150 sccm. (a)  $[e]$ , (b)  $[\text{Cl}^-]$ , and (c) electron temperature. The electron density reaches a quasisteady state for duty cycles  $>30\%$  and decays several orders of magnitude during the afterglow.

trons. At this time, the  $[\text{Cl}^-]$  begins to decrease due to ion-ion neutralization and diffusion. The latter is enabled by the system transitioning to an ion-ion plasma.<sup>12</sup>

$[\text{Cl}^-]$  continues to decrease well into the power pulse. As  $T_e$  peaks at the leading edge of the power pulse, while the electron density is still low, the rate of attachment decreases while the rate of nonattaching electron impact dissociation increases, resulting in a decrease in  $[\text{Cl}^-]$ . At  $\approx 20 \mu\text{s}$  into the activeglow,  $T_e$  decreases to  $\approx 3.0 \text{ eV}$ , corresponding to its value during cw operation. The lower  $T_e$  decreases rates of nonattaching electron impact dissociation and increases the rate of dissociative attachment, and so  $[\text{Cl}^-]$  increases.

The reactor averaged  $n_e$ ,  $[\text{Cl}^-]$  and  $T_e$  are shown in Fig. 15 for PRFs of 5, 10, and 20 kHz for a constant peak power of 300 W and duty cycle of 50%. As the PRF is lowered to 5 kHz, a quasisteady state for  $n_e$  and  $T_e$  is obtained during the longer activeglow. However, as the power

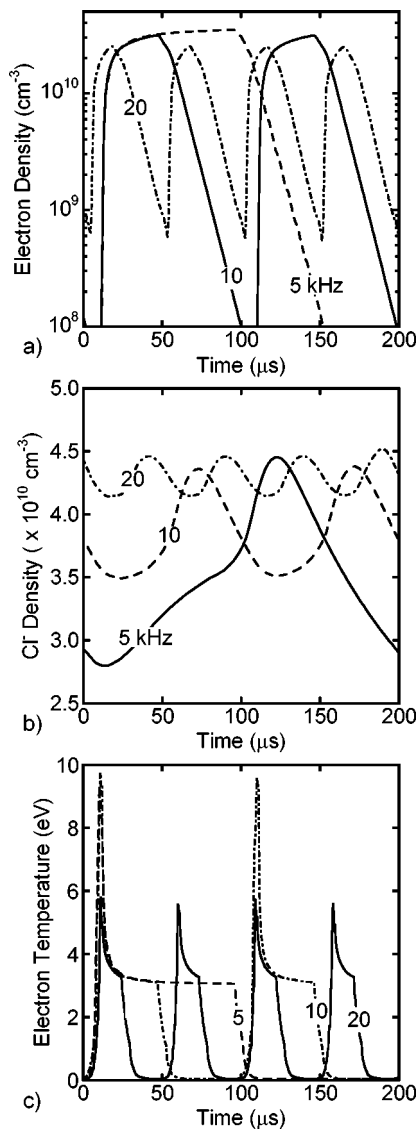


FIG. 15. Reactor averaged plasma properties in  $\text{Cl}_2$  as a function of time for different PRFs for a constant peak power of 300 W, duty cycle of 10 kHz and gas flow of 150 sccm. (a)  $[e]$ , (b)  $[\text{Cl}^-]$  density, and (c) electron temperature.

remains off for a longer duration at lower PRFs,  $n_e$  decays to lower values by the start of the next power pulse. As a result, there is a correspondingly higher peak in  $T_e$  at the leading edge of the power pulse. At lower PRFs, the afterglow is also long enough that the  $[\text{Cl}^-]$  has an opportunity to decay by diffusion during the longer ion-ion phase. The plasma potential decays to a sufficiently small value to enable diffusion losses to dominate over the production of  $\text{Cl}^-$  ions by dissociative attachment by the depleted electrons.

The positive ion and Cl densities above the wafer (height-B) averaged over a pulse period at the end of six pulses following cw operation are shown in Fig. 16. Values are shown for duty cycles of 30%–70% (peak power 300 W, 150 sccm, 10 mTorr, 10 kHz). As the peak power during the activeglow is constant, the time averaged positive ion density increases with increasing duty cycle and increasing average power. As the duty cycle is decreased, the longer afterglow period enables mitigating diffusion to more efficiently

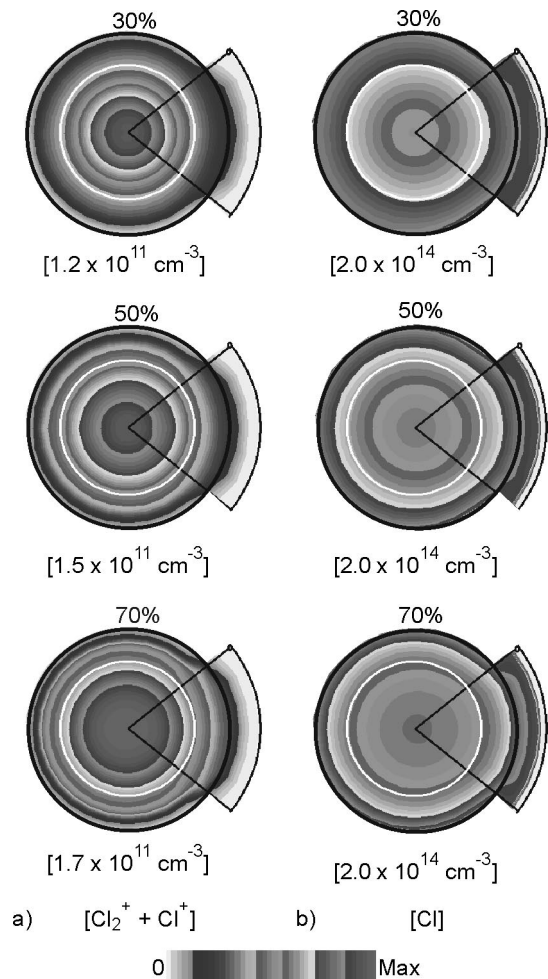


FIG. 16. Plasma parameters in  $\text{Cl}_2$  above the wafer (height-B) at the end of six pulses following cw operation for duty cycles of 30%, 50%, and 70% (peak power of 300 W, 10 mTorr, 150 sccm, and PRF of 10 kHz). (a) Positive ion density ( $[\text{Cl}_2^+] + [\text{Cl}^+]$ ) and (b)  $[\text{Cl}]$ . The white circle is the outline of the substrate. The maximum for each quantity is noted in the brackets. Lower duty cycles resulted in better azimuthal symmetry provided that the afterglow is long enough for electrons to be depleted by attachment.

smoothen of the radical and ion densities. As a result, the Cl density becomes more azimuthally uniform at lower duty cycles.

Highly thermal electron attaching chemistries such as  $\text{Cl}_2$  tend to be more sensitive to pulsing as a method of improving uniformity than are electropositive plasmas. For example, comparing the plasma parameters for cw operation in Fig. 13 with pulsed operation in Fig. 16, any degree of pulsing which significantly depletes the electrons during the afterglow will break the positive feedback cycle which occurs through the residual nonuniform plasma conductivity. The fact that attachment dominates electron loss during the afterglow results in any residual electrons generally being more uniform. For 30% and 50% duty cycles, the electrons are significantly depleted in the afterglow and the resulting uniformity is similar. For a 70% duty cycle having a correspondingly shorter afterglow period, the electrons are less depleted in the afterglow, thereby leaving an asymmetric imprint of the positive feedback from the longer activeglow period. This results in larger pulse averaged asymmetries.

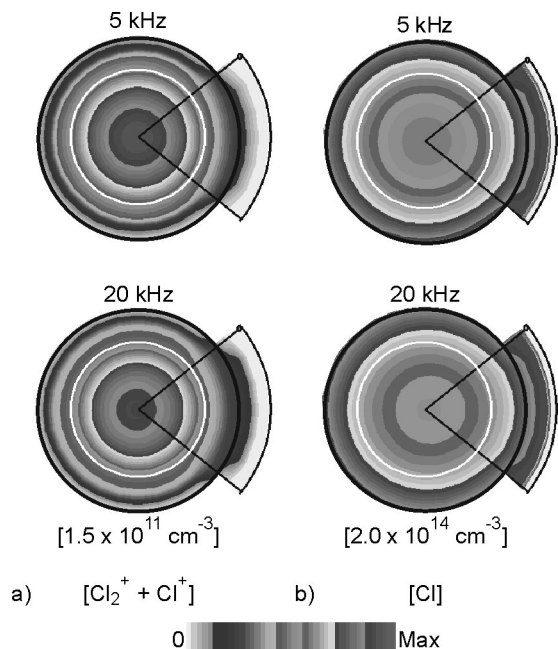


FIG. 17. Plasma parameters in  $\text{Cl}_2$  above the wafer (height-B) averaged over a pulse period at the end of six pulses for 5 and 20 kHz (peak power of 300 W, 10 mTorr, 50 sccm, and duty cycle of 50%). (a) Positive ion density ( $[\text{Cl}_2^+] + [\text{Cl}^+]$ ) and (b)  $[\text{Cl}]$ . Lower PRFs resulted in more uniform species densities at the plane above the wafer.

Moderately attaching gas chemistries, such as  $\text{CF}_4$  in which pulsing typically does not completely deplete the electron density during the afterglow are not so sensitive.

The positive ion and Cl radical densities above the wafer (height-B) averaged over a pulse period at the end of six pulses for PRFs of 5 and 20 kHz are shown in Fig. 17 (peak power 300 W, 150 sccm, 10 mTorr, 50%). The increased afterglow times for lower duty cycles result in improved symmetry. The uniformity in species densities improved by  $\approx 15\%$  as the PRF was reduced from 20 to 5 kHz. The uniformity in power deposition correspondingly improved by 20% and uniformity in electron impact ionization sources improved by 10%. These scalings reflect that  $n_e$  is more depleted at lower PRFs due to the longer afterglow periods.

## V. CONCLUDING REMARKS

cw operation of ICP reactors with flow asymmetries resulting from pumping can produce asymmetric plasma parameters due to a positive feedback loop between non-

uniform plasma conductivity and power deposition. Pulsed plasma operation of ICPs can reduce this feedback and, hence, can be employed as a potential method for reducing azimuthal asymmetries. A moderately computationally parallel 3D model was employed to investigate the pulsed operation of Ar and  $\text{Cl}_2$  ICPs. We found that diffusion during the afterglow between pulses smoothens the species density. As the electron density at the end of the afterglow becomes more symmetric, the power deposition during subsequent pulses is more uniform. In Ar ICPs, the azimuthal uniformity of plasma parameters generally improved relative to cw operation when decreasing duty cycle or PRF due to the longer afterglow period, although these improvements were not necessarily monotonic. Similar improvements were also observed in  $\text{Cl}_2$  pulsed ICPs. As dissociative attachment dominates in the afterglow of  $\text{Cl}_2$  pulsed plasmas, it provides a more uniform sink for electrons during the afterglow compared to ambipolar diffusion, and so these highly electronegative plasmas have uniformities that are more sensitive to pulsing.

## ACKNOWLEDGMENTS

This work was supported by the National Science Foundation (CTS99-74962, CTS03-15353), the Semiconductor Research Corporation, and Applied Materials Inc.

- <sup>1</sup>J. Hopwood, *Plasma Sources Sci. Technol.* **1**, 109 (1992).
- <sup>2</sup>J. H. Keller, *Plasma Sources Sci. Technol.* **5**, 166 (1996).
- <sup>3</sup>U. Kortshagen, A. Maresca, K. Orlov, and B. Heil, *Appl. Surf. Sci.* **192**, 244 (2002).
- <sup>4</sup>T. Makabe and Z. L. Petrovic, *Appl. Surf. Sci.* **192**, 88 (2002).
- <sup>5</sup>Z. L. Petrovic and T. Makabe, *Mater. Sci. Forum* **282–283**, 47 (1998).
- <sup>6</sup>M. H. Khater, L. J. Overzet, and B. E. Cherrington, *J. Vac. Sci. Technol. B* **16**, 490 (1998).
- <sup>7</sup>T. A. Kim and E. S. Aydil, *J. Appl. Phys.* **92**, 6444 (2002).
- <sup>8</sup>T. A. Kim, S. J. Ullal, V. Vahedi, and E. S. Aydil, *Rev. Sci. Instrum.* **73**, 3494 (2002).
- <sup>9</sup>T. Panagopoulos, D. Kim, V. Midha, and D. Economou, *J. Appl. Phys.* **91**, 2687 (2002).
- <sup>10</sup>D. J. Economou, T. L. Panagopoulos, and M. Meyyappan, *Micro* **16**, 108 (1998).
- <sup>11</sup>P. Subramonium and M. J. Kushner, *J. Vac. Sci. Technol. A* **20**, 313 (2002).
- <sup>12</sup>P. Subramonium and M. J. Kushner, *J. Vac. Sci. Technol. A* **20**, 325 (2002).
- <sup>13</sup>R. L. Kinder, A. R. Ellingboe and M. J. Kushner, *Plasma Sources Sci. Technol.* **12**, 561 (2003).
- <sup>14</sup>Kuck and Associates, <http://www.kai.com/parallel/kappro/>.
- <sup>15</sup>D. P. Lymberopoulos and D. J. Economou, *J. Res. Natl. Inst. Stand. Technol.* **100**, 473 (1995).
- <sup>16</sup>J. N. Bardsley and J. M. Wadehra, *Phys. Rev. A* **20**, 1398 (1979).